Benha Journal of Applied Sciences (BJAS) **print: ISSN 2356–9751**
Vol. (7) Issue (5) (2022), (269-279) **online: ISSN 2356–976x**
http://bjas.journals.ekb.eg

Auto-combustion synthesis and characterization of zirconium oxide nanoparticles for removal of crystal violet dye from aqueous solution

***Rowaida M. Fahmy, Sayed A. Shama, Abdel-Azem M. El-Sharkawy, and Ayman A. Ali**
*Chemistry Department, Faculty of Science, Benha University, Benha, Egypt.
E-mail: rowaidamahmmoud@yahoo.com

Abstract

In the present work, zirconium oxide nanoparticles were synthesized via auto-combustion method using urea. Fourier transform infrared spectroscopy (FTIR), X-Ray diffractometry (XRD), High resolution transmission electron microscopy (HR-TEM) as well as Field emission scanning electron microscopy (FE-SEM) were used to elucidate the structure and morphology of the synthesized zirconium oxide nanoparticles. The synthesized ZrO_2 nano-adsorbents were used for crystal violet removal from aqueous solution. Various parameters were checked in a batch method for the adsorption process of crystal violet dye on zirconium oxide adsorbents such as pH solution, duration time, ZrO_2 dose (adsorbents), initial dye concentration as well as temperature. The adsorption kinetics, isotherm models and thermodynamic parameters were discussed.

Keywords: ZrO_2 nanoparticles; Auto-combustion method; Adsorption process; Thermodynamics

1. Introduction

Organic and inorganic contaminants are significant issues of water pollution due to their harmful effect, severe toxicities and carcinogenic nature [1]. Petroleum wastes, wood type materials, tannin-rich materials, fertilizer wastes, zeolites, sugar industry wastes, organic dyes, chitosan, seafood processing wastes were the main types of wastes well as ore minerals [2]. Cationic dyes, being as the most dangerous one than other dyes, are commonly used in the industry. Crystal violet (CV) dye is an example of cationic dye, used in many industries such as paper, textiles, printing inks and pharmaceuticals ones [3]. If (CV) dye presents in water, reduction of sunlight penetration and prevention of photosynthesis process [4]. In addition, (CV) dye in definite concentrations can cause several diseases such as blindness , respiratory failure, eye irritation, heart rate abnormalities, skin irritation, cyanosis and tumors [3].

There were many methods used for water treatment such as microbial decomposition, oxidation, coagulation, reverse osmosis, ion exchange, photo-catalytic degradation, electro-dialysis, electrolysis as well as adsorption [5, 6]. Low cost, nonexistence of harmful residues and ease of operation distinguished adsorption method among various water treatment ones [7-13]. ZrO_2 has attracted considerable attention due to its usage in industrial and medical applications such as fire- and heat-resistant material, wide band-gap semiconductor material, catalyst, solid oxide fuel cell , oxygen sensors, dental and body implants and ceramic biomaterial owing to its remarkable physical properties, such as high melting point, high strength, good toughness, corrosion resistance and low thermal conductivity [14-17]. The principle target of this work is the removal of crystal violet from industrial wastewater streams using ZrO_2 nanoparticles before entering the environment.

2. Materials and methods

2.1. Materials and chemicals

Zirconium Oxynitrate octahydrate ($ZrO(NO_3)_2 .8H_2O$, 99%), was purchased from Alpha Chemika company. Crystal violet or methyl violet 10B ($C_{25}H_{30}ClN_3$, 99%) was purchased from Sigma–Aldrich chemical company. Urea (CH_4N_2O, 99.5%), Hydrochloric acid (HCl, 30-34%), Sodium Hydroxide (NaOH, 99%), Nitric acid (HNO_3, 69%) and Ammonium Hydroxide (NH_4OH, 33%) were brought from El-Nasr for pharmaceutical and chemical company. All materials and chemicals with the highest quality and used directly.

2.2. Auto-combustion synthesis of zirconium oxide nanoparticles

The required amounts of zirconium oxynitrate octahydrate (oxidant) and that of urea (reducer) were calculated accurately and dissolved separately in 25 mL of bidistilled water. Zirconium salt solution was stirred well for 30 minutes for complete dissolution. Using a pH meter, adjust the pH of a solution at pH 9 using NH_4OH until the precipitation occurred as evidence of zirconium oxyhydroxide formation. The synthesized zirconium oxyhydroxide was precipitated, collected, washed several times using bidistilled water and finally centrifuged at 3500 rpm for 10 minutes to separate the synthesized precipitate. 10 mL concentrated HNO_3 and 25 mL bidistilled water was added to the previous precipitate and stirred with a hotplate/stirrer for 1 hour at 150 ^oC. At this temperature, solution volume reduced immediately until reached 25 mL. Let the solution cool, then urea fuel solution was added to it and stirred well for 30 minutes obtaining a homogeneous mixture. The solution was ignited at 300 ^oC, resulting in the release of different gases and the obtained nanoparticles were found in pale white color. The nanoparticles seemed to be impure, so, the powder was annealed at 600 °C for 2 hours in a muffle furnace, forming pure nanocrystalline zirconium oxide ZrO_2 labelled as (ZU) according to chemical Eq. (1).

$$\mathbf{6ZrO(NO_3)_2.8H_2O + 10CH_4N_2O \rightarrow 6ZrO_2 + 16N_2 + 10CO_2 + 20H_2O} \quad \textbf{(1)}$$

2.3. Characterization

The ZrO_2 nanoparticles (ZU sample) were recognized by (FTIR) spectroscopy which was tested with a Perkin-Elmer instrument to examine the structure of the fabricated (ZU sample). For structural analysis, X-ray Diffraction patterns were measured. (Bruker; model D8 advance) with monochromatic Cu-Kα_1 radiation, 1.54178 (A^o) in the angular range of 10-70^o with step size 0.02^o (2Ɵ) and scan step time 0.4 (s). Scanning Electron Microscopy of the (ZU sample) was carried out on an (FE-SEM, Zeiss Sigma 500 VP) to estimate the characteristics surface of the (ZU sample). The images of TEM are used for the description of the morphology and the crystalite size of the (ZU sample). These were revealed using High-resolution transmission electron microscopy: HR-TEM (model Tecnai G20, FEI, Netherland) with an electron voltage of 200 kV.

2.4. Adsorption studies

The Batch technique was carried out to achieve the optimum operating conditions for elimination and separation of (CV) dye on zirconium nanoparticles. Different parameters such as solution pH (2–9), ZrO_2 nanoparticles dosage (0.01–0.125 g/L), initial (CV) dye concentration (10–100 mg/L), duration time (5–200 min) and interfering salt (0- 0.1 g/L KCl). To carry out the adsorption experiments, 25 mL of (CV) dye solution was taken by adding an optimized adsorbent dose of 0.05 g. The solution pH was adjusted with 0.1 M HCl /or 0.1 M NaOH solutions and the mixture was stirred well. Various samples of crystal violet (CV) dye were separated from the fabricated solutions at constant conditions and contact time, and thereafter dye samples were centrifuged. The final concentration of (CV) dye in the clear solution was estimated at λ_{max} = 573 nm by double beam UV–Vis spectrophotometer. The percentage removal (PR %) of (CV) dye and adsorption capacity (q_t) were calculated using the following Eq. (2, 3) :

$$\mathbf{PR\ \% = (W_o - We)/W_o \times 100} \quad \textbf{(2)}$$

$$\mathbf{q_t = (W_o - W_t)(V/m)} \quad \textbf{(3)}$$

Where q_t is the adsorption capacity of (CV) dye adsorbed on zirconium oxide nanoparticles at the time of equilibrium (mg/g), W_o and W_e are the initial and final concentration of (CV) dye (mg/L), V is the volume of sample, and m is the mass of adsorbent. Finally, besides percentage removal (PR %) of (CV) dye and adsorption capacity (q_t), isotherm, thermodynamic studies and adsorption kinetics were performed under the variable experimental parameters.

3. Results and discussion

3.1. Characterization of ZrO_2 nanoparticles

FTIR spectroscopy is a beneficial tool to investigate the chemical structure and the active groups of the synthesized nanoparticles. Figure (1) showed the (FTIR) spectra of the annealed powder of ZrO_2 nanoparticles (ZU sample) in the range of the wavenumber (400-4000 cm^{-1}). The major bands in the range of 500-800 cm^{-1} (at 530, 600, 580, 700, 780 cm^{-1}) in the spectra, are related to the tetragonal and monoclinic structure of the obtained ZrO_2 stretching vibration modes. The broadband at 3442 cm^{-1} and the sharp band at 1639 cm^{-1} corresponded to the stretching and bending mode of hydroxyl groups (O-H) or/and water molecules on the surface of the synthesized ZrO_2 nanoparticles [18-21].

The crystalline structure of ZrO_2 nanoparticles (ZU sample) was investigated using (XRD) and the obtained result was manifested in Figure (2). The data extracted from the pattern of zirconium oxide nanoparticles (ZU sample) reflected the appearance of the tetragonal and monoclinic crystal structure according to the reference cards No. 01-079-1771 and 00-036-0420. The sharp diffraction peaks at 2θ value of 30.2, 34.4, 35.169, 50.273, 50.8, 59.349 and 60.2 correspond to the (101), (002), (110), (112), (220), (103) and (211) planes. Also, the diffraction peaks at 2θ value of 28.245, 31.467, 35.308 and 50.120 correspond to the (-111), (111), (200) and (-220) planes [22-28]. The crystallite size (CS, nm) of the obtained ZrO_2 nanoparticles (ZU sample) can be extracted by using the Scherrer eq. (4):

$$\mathbf{CS = Z\lambda/\beta\cos\theta_B} \quad \textbf{(4)}$$

Where λ is the wavelength of X-ray radiation, Z is constant, β is the full width at half the maximum of the diffraction peak and θ_B is the Bragg diffraction angle. The calculated average particle size of the annealed zirconium oxide nanoparticles (ZU sample) is found to be 16.8 nm.

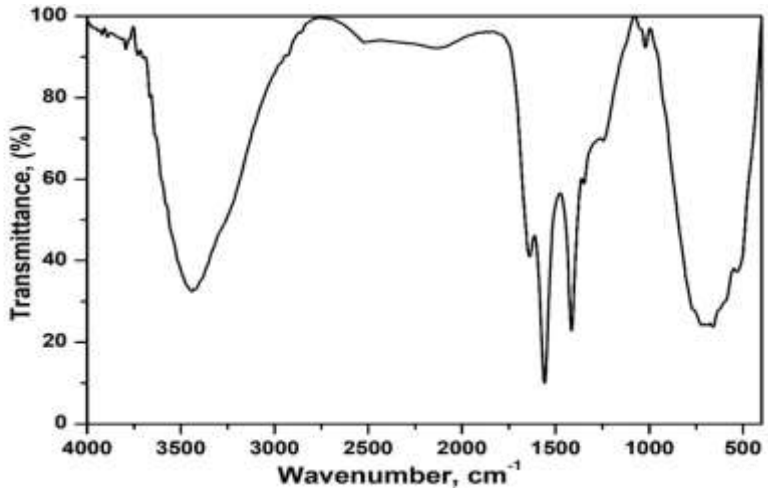

Fig. (1) FTIR of ZrO_2 nanoparticles (ZU sample) using auto-combustion method and urea as a fuel.

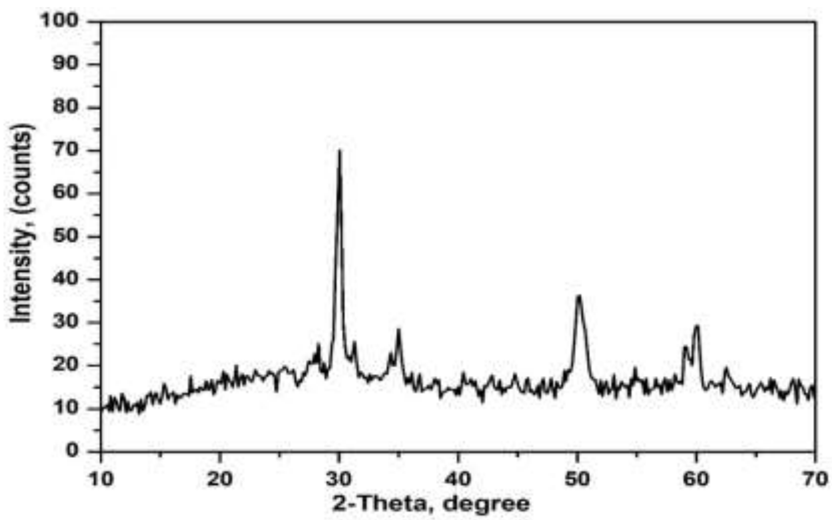

Fig. (2) XRD of ZrO_2 nanoparticles (ZU sample) using auto-combustion method and urea as a fuel.

The surface and bulk morphologies of the calcination zirconium oxide nanoparticles (ZU sample) were investigated using (HR-TEM) and (FE-SEM) as shown in Figure 3(a-d). The choice of urea as organic fuel has an effective role in both particle size and bulk morphology of the obtained zirconium oxide as clarified in Figure 3(a and b). From the TEM images, zirconium oxide nanoparticles showed an incompletely spherical shape with soft agglomeration and particle size calculated from the micrograph to be 21 nm. The surface morphology and the grain size of the obtained ZrO_2 nanoparticles (ZU sample) were tested by using scanning electron microscopy as shown in Figure 3(c and d). The micrographs of the fabricated zirconium oxide nanoparticles (ZU sample) showed the formation of a sheet and tetragonal shape with large single grains and boundaries are very clearly visible. The obtained grain size of the (ZU sample) from SEM micrographs was 130 nm and this value reflected the hard agglomeration of the grains on the surface of the formation of zirconium oxide nanoparticles [22].

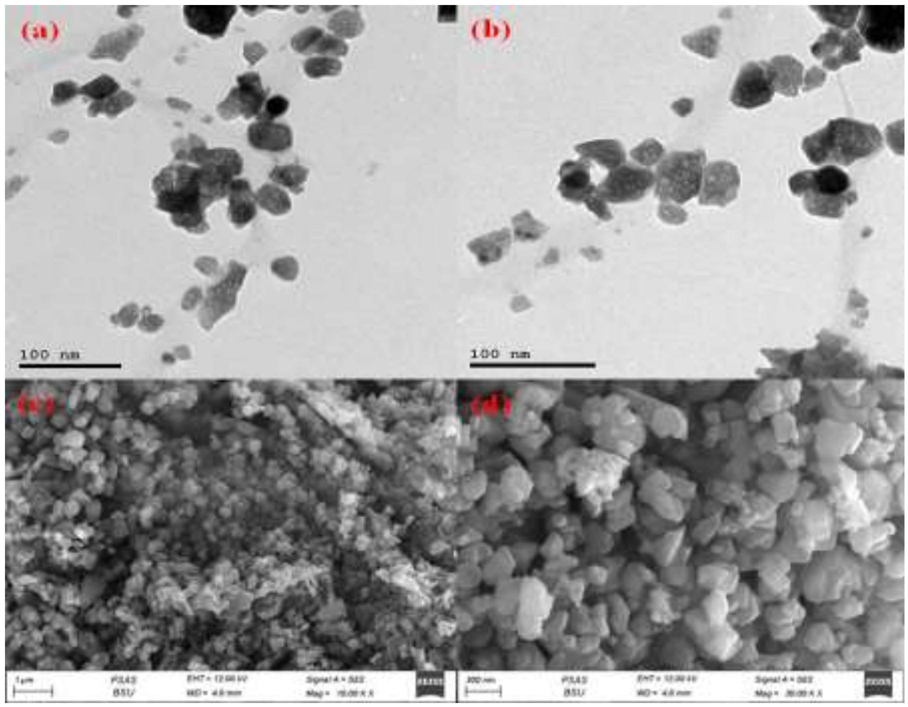

Fig. (3) HR-TEM (a and b) and FE-SEM (c and d) of zirconium oxide nanoparticles (ZU sample).

3.2. Batch adsorption experiments

pH solution is a very valuable parameter in the dye adsorption process, as it controls the type of electrostatic charges that are gained by the charged dye species. For this, pH effect of the adsorption process of crystal violet (CV) on ZrO_2 nanoparticles (ZU sample) was studied by observing the percentage removal of 25 mL of 50 mg/L from (CV) dye in the pH range of 2–9. The maximum dye removal percentage (PR % = 87) was observed at pH 8 for the removal of (CV) dye on the (ZU sample), as manifested in Figure 4(a). The removal and dye adsorption were observed in alkaline medium due to the formation of the planar ring in triphenylmethane groups, yielding the carbinol as a new material [29].

Duration time is one of the significant factors in the adsorption process which clarify the interaction between the adsorbent surface of the (ZU sample) and the (CV) dye. contact time effect of (CV) dye adsorption efficiency using ZrO_2 nanoparticles (ZU sample) as adsorbents was investigated using 25 mL of 50 mg/L of (CV) dye at pH 8 in the time range of (5–200 min) and the result was manifested in Figure 4(b). According to the obtained result, the removal of (CV) dye was increased with increasing time using ZrO_2 nanoparticles (ZU sample): PR% =54.5, Q_m = 13.6 mg/g until equilibrium occurred at 180 min [30] .

Absorbents dose is a remarkable parameter which can affects the efficiency and adsorption capacity of the (ZU sample) as an adsorbents for (CV) dye. The effect of the adsorbent amount of the (ZU sample) on adsorption efficiency and capacity was investigated using ZrO_2 nanoparticles (ZU sample) in the range of 0.01–0.125 mg and 25 ml of 50 mg/L of (CV) dye at pH 8 and 180 min. The result in Figure 4(c) was manifested that with increasing the adsorbents dose of the (ZU sample), the adsorption percentage increased from 40 % to 51% which was due to the available and unsaturated active sites [31].

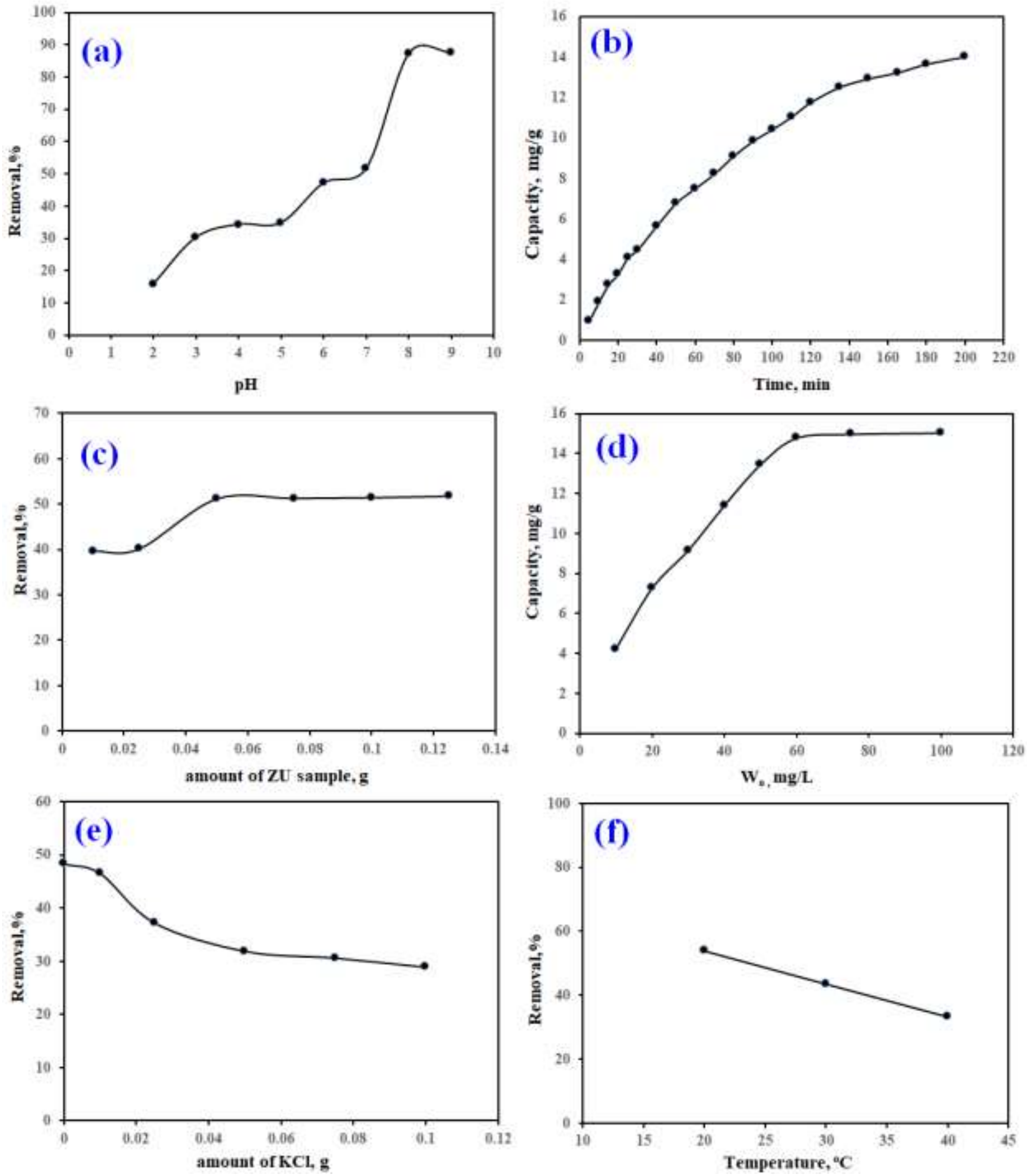

Fig. (4) Effect of pH (a), time (b), ZU amount (c), initial dye concentration (d), amount of salt (e) and temperature (f) for the adsorption of the (CV) dye using the zirconium oxide nanoparticle (ZU sample).

The concentration of (CV) dye is an effective parameter in the elimination process. It is tested using 25 mL of (10-100) mg/L of (CV) dye and 0.05 g of ZrO_2 (ZU sample) at pH 8 and 180 min. From Figure 4(d) it was found that the capacity of zirconium oxide nanoparticles (ZU sample) increased with increasing the (CV) dye concentration till it recorded 14.8 mg/g, 15.7 mg/g and 16.4 mg/g for initial concentration 60 mg/L, 80 mg/L and 100 mg/L respectively. The adsorption increased after a certain equilibrium concentration at 60 mg/L. The values of adsorption capacity became constant as the initial dye concentration increased. It needs to be the driving force to overcome the resistance of the mass transfer of (CV) dye solution (liquid phase) to the surface of the solid (ZU sample) [32].

The effect of conflicting salt was studied by the volume: 25 mL of 50 mg/L of (CV) dye, 50 mg of (ZU sample) at pH 8 and 180 min. various amounts of KCl in the range of (0 - 0.1 mg) as interfering salt are used and the data were shown in Figure 4(e). It was reflected that the addition of amounts of KCl lead to low removal values of (CV) dye, and decreased the adsorption capacity of the (ZU sample) as a result for competing between conflicting salt and (CV) dye for active sites on ZrO_2 oxide nanoparticles. [33] .

The temperature of adsorption solution effect on the removal of (CV) by ZrO_2 nanoparticles (ZU sample) was studied at three different temperatures 293 K, 303 K and 313 K to elucidate the removal process. The data extracted that the adsorption capacity decreased as the temperature increased for the removal of (CV) dye on the ZrO_2 nanoparticles (ZU sample) which is exhibited in Figure 4(f) which is a result of destruction of physical bonds between (CV) dye and ZrO_2 nanoparticles. It indicates that the removal of (CV) dye on the synthesized zirconium oxide nanoparticles (ZU sample) was an exothermic process [30].

3.4. Adsorption isotherm models

Models of adsorption isotherm were used to investigate the crystal violet (adsorbate) molecules adsorbed at ZrO_2 surface (ZU sample: adsorbent) when concentration of adsorbate reaches in equilibrium state and also describe the adsorption capacity of adsorbent. To examine the isotherm models of crystal violet dye adsorption onto the ZrO_2 nanoparticles (ZU sample), the theories of Langmuir, Freundlich, and Temkin respectively were applied. The high coefficients of determination value (R^2) express the best fitting. The linear form of Langmuir Freundlich, and Temkin isotherms [34-37] model as displayed in Figure 5(a-c) and the three models are given by Eq. (5-7) as the following:

$$\mathbf{\frac{W_e}{Q_e} = \frac{1}{K_L\,Q_m} + \frac{W_e}{Q_m}} \qquad (5)$$

$$\mathbf{\ln Q_e = \ln K_F + \frac{1}{P}\ \ln W_e} \qquad (6)$$

$$\mathbf{Q_e = G\ln K_T + G\ln W_e} \qquad (7)$$

Where W_e is the equilibrium concentrations of crystal violet (CV) dye in solution, Qe is the equilibrium adsorption capacity of (CV) dye using ZrO_2 (ZU sample) as adsorbents, K_L is the Langmuir parameter, K_f is the Freundlich constant, (1/P) is the heterogeneity factor, Q_m is the maximum quantity of adsorbed solute to adsorbent. G is constant (G= RT/X), K_T is Temkin equilibrium constant due to the maximum binding energy and X is related to the heat of adsorption.

By applying the previous theories of isotherm (Langmuir, Freundlich and Temkin models) on the adsorption of crystal violet (CV) dye using the synthesized ZrO_2 nanoparticles (ZU sample), the experimental data shown in Table (1). It revealed that the Langmuir model fits well (R^2 = 0.9914) than the Freundlich model (R^2=0.979).The theoretical and experimental adsorption capacities determined from Langmuir model to be 18.52 mg/g and 13.6 mg/g respectively. The values of R_L were found to be 0.46178-0.07902 which is corresponded to the initial concentration (10-100 mg/L). These values reflected that the adsorption process of the crystal violet dye (CV) on the (ZU sample) is a favorable process. Due to the value of X constant from Temkin model, the heat of adsorption (X) determined to be 0.6931 KJ/mole which reflected that the weak interaction force between the synthesized (ZU sample) and crystal violet dye (CV).

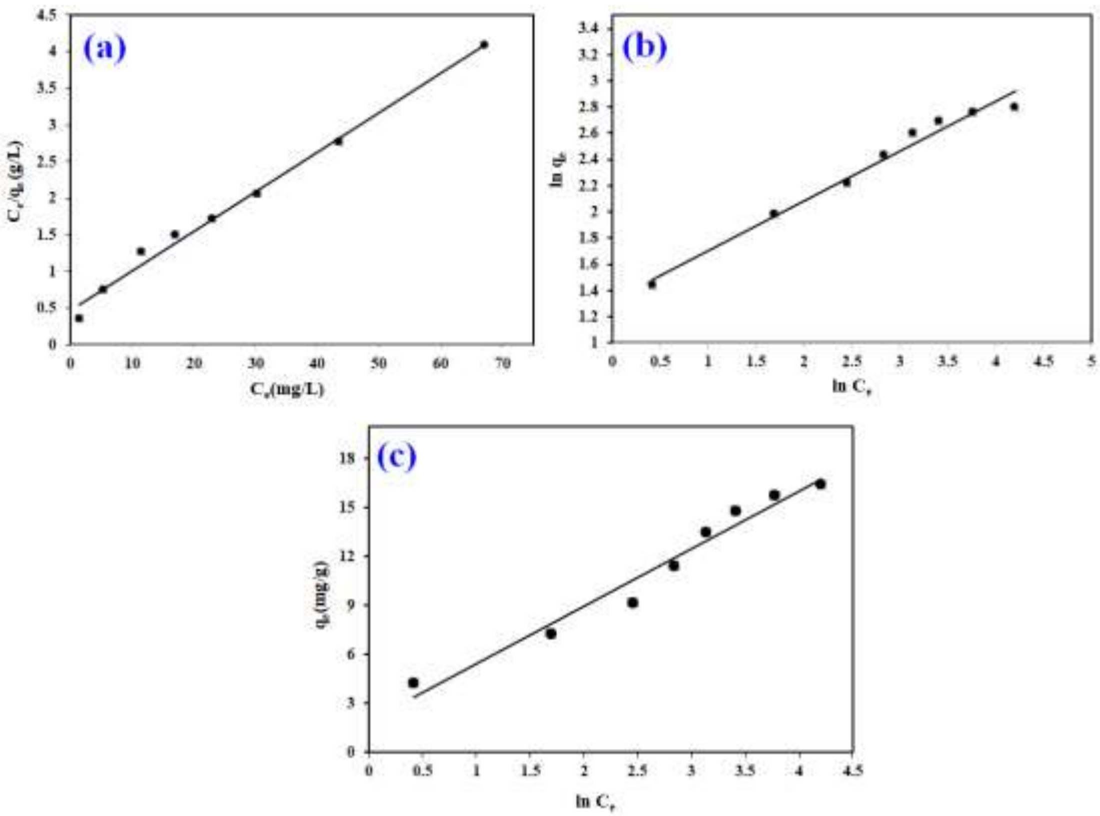

Fig (5) Langmuir (a), Freundlich (b) and Temkin (c) models for (CV) dye removal on zirconium oxide nanoparticles (ZU sample).

Table (1) Langmuir, Freundlich, and Temkin isothermal constants for (CV) adsorption on zirconium oxide nanoparticles (ZU sample).

Adsorption isotherm	Constants	Values
Langmuir	K_L (L/mg)	0.11656
	$Q_{m\,(cal)}$ (mg/g)	18.52
	R_L	0.46178-0.07902
	R^2	0.9914
	$Q_{m\,(exp)}$ (mg/g)	13.6
Freundlich	K_F [(L/mg) (L/mg)$^{1/n}$]	3.7678
	$Q_{m\,(cal)}$ (mg/g)	17.8
	P (L/mg)	2.639
	R^2	0.979
	$Q_{m\,(exp)}$ (mg/g)	13.6
Temkin	K_T (L/mg)	1.730
	X (J/mol)	0.6931
	G	3.5147
	R^2	0.9651

3.5. Adsorption kinetics

Pseudo first order and also pseudo second order in addition to intra-particle diffusion models were described the adsorption kinetics as shown in Eq. (8-10). The experiments was examined at time intervals varied from the 0 to 200 min at constant temperature, 50 mg of (ZU sample) and 50 mg/L of crystal violet (CV) dye as manifested in Figure 6(a-c) [38].

$$\mathbf{\log(Q_e - Q_t) = \log Q_e - \frac{K_1 t}{2.303}} \quad (8)$$

$$\mathbf{\frac{t}{Q_t} = \frac{1}{K_2 {Q_e}^2} + \frac{t}{Q_e}} \quad (9)$$

$$\mathbf{Q_t = K_{IPD} t^{0.5} + Y} \quad (10)$$

Where Q_e and Q_t are the amounts of crystal violet (CV) dye adsorbed at equilibrium and time t (min), respectively and k_1 is the pseudo first order rate constant of adsorption, k_2 is pseudo second order rate adsorption constant, k_{IPD} is intra-particle diffusion constant and Y is constant. As shown in Table (2) and according to the magnitude of R^2, the pseudo-second-order model is the best fitting for the adsorption of crystal violet (CV) dye on the ZU nano-adsorbents. The removal of crystal violet (CV) dye on zirconium oxide nanoparticles (ZU sample) follows the pseudo-second-order model (R^2=0.995) as displayed in Figure 6(a-b). The values of theoretical and experimental adsorption capacities of crystal violet (CV) on zirconium oxide nano-adsorbents (ZU sample) were 22 mg/g and 13.6 mg/g respectively. Figure 6(c) explains the intra-particle diffusion type and the values determined from linear relation. The experimental plots didn't pass through the origin, and it is reflected that the intra-particle diffusion is not the only model for explaining the adsorption mechanism of the of the crystal violet (CV) dye on the zirconium oxide nano-adsorbents (ZU sample).

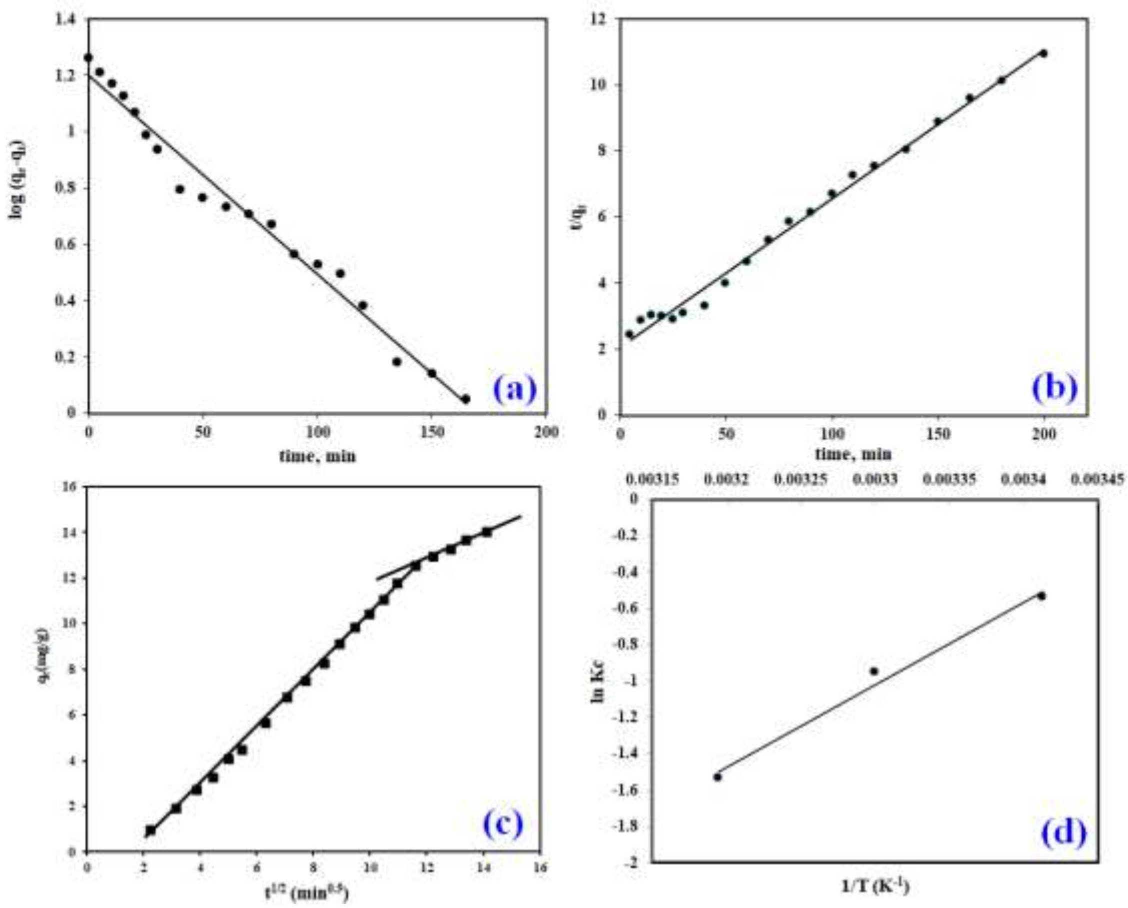

Fig. (6) Pseudo-first-order (a), pseudo-second-order (b), intra-particle diffusion (c) and linear relation of Van't Hoff (d) for the removal of (CV) dye on (ZU sample).

Table (2) Adsorption kinetic parameters of the removal of crystal violet (CV) dye on zirconium oxide nanoparticles (ZU sample).

Model		Parameters	Values
Pseudo first order		$K_1(min^{-1})$	0.01799
		$q_{m\ (cal)}$ (mg/g)	16.77
		R^2	0.962
		$q_{m\ (exp)}$ (mg/g)	13.6
Pseudo second order		K_2(g/mg.min)	0.00039
		$q_{m\ (cal)}$ (mg/g)	22
		R^2	0.9949
		$q_{m\ (exp)}$ (mg/g)	13.6
Intra-particle diffusion	**(I)**	K_i (mg/g $min^{0.5}$)	1.245
		C (mg/g)	-2.10
		R^2	0.998
	(II)	K_i (mg/g $min^{0.5}$)	0.779
		C (mg/g)	0.3192
		R^2	0.9619

3.6. Thermodynamics study

Thermodynamic parameters such as enthalpy (ΔH°) and entropy (ΔS°) in addition to Gibb's free energy (ΔG°) can be calculated for the removal of (CV) by ZrO_2 nano adsorbents (ZU sample) from the following Eq. (11, 12) [11].

$$\ln K_c = \frac{\Delta S^\circ}{R} - \frac{\Delta H^\circ}{RT} \qquad (11)$$

$$\Delta G^\circ = \Delta H^\circ - T\Delta S^\circ \qquad (12)$$

Where ΔG°, ΔH° and ΔS° are Gibb's free energy change, enthalpy change and entropy change respectively. The k_c (equilibrium constant: L/g) values were calculated from q_e/C_e, T is the temperature in Kevin (k) and R is the gas constant. The plot of $\ln(k_c)$ against 1/T appeared as linear relation of Van't Hoff shown in Figure 6(d) with slope (-ΔH°/R) and intercept (ΔS°/R) and hence ΔG° can be calculated. Table (3) summarized the experimental parameters for the removal of (CV) by ZrO_2 nano-adsorbents (ZU sample).

The negative value of ΔH° revealed that the adsorption process is exothermic one beside this; its value was lower than 40 KJ/mol so, the removal of crystal violet (CV) dye on the synthesized ZrO_2 nano-adsorbents was a physical process. The positive value of ΔG° expressed the non-spontaneously behavior of the adsorption process which was unfavorable at high temperatures. The negative value of ΔS° reflected the decreasing in the degree of freedom of solution for the adsorption process.

Table (3) Thermodynamic parameters for the (CV) adsorption on zirconium oxide nanoparticles (ZU sample).

Temp, K	Thermodynamic parameters		
	ΔG° (KJ/mol)	**ΔH° (KJ/mol)**	**ΔS° (KJ/mol)**
293	1.2334	-37.8623	-0.13343
303	2.5677		
313	3.9020		

Conclusion

Auto-combustion method was used for the fabrication of zirconium oxide nanoparticles (ZU sample) using urea as fuel. ZrO_2 nanoparticles were prepared after the calcination at 600 °C for 2h. (ZU sample) as nano absorbent was used for removal of cationic dye crystal violet (CV) from aqueous solution. The adsorption process was non-spontaneous, exothermic and unfavorable at high temperatures.

Acknowledgements

The authors express their great thanks to Chemistry Department, Faculty of Science, Benha University, Egypt for great helping us with completing the current research.

References

[1] M. Ismail1 , K. Akhtar , M.I. Khan , T. Kamal , M. A. Khan , A. M. Asiri , J. Seo and S. B. Khan, Pollution, Toxicity and Carcinogenicity of Organic Dyes and their Catalytic Bio-Remediation. Curr. Pharm. Des.,Vol.(25), PP. 3653-3671, 2019.

[2] I. Ali, A. Tabrez, T. Khan, Low cost adsorbents for the removal of organic pollutants from wastewater. J. Environ. Manage., Vol.(113), PP. 170-183, 2012.

[3] S. P. Fakhri, S. Jamaleddin, R. Foroutan, N. Arsalani and B. Ramavandi, Crystal violet dye sorption over acrylamide/graphene oxide bonded sodium alginate nanocomposite hydrogel. Chemosphere,Vol.(270), PP. 129419, 2021.

[4] H. Mittal, A. A. Alili, P. P. Morajkar and S. M. Alhassan, Graphene oxide crosslinked hydrogel nanocomposites of xanthan gum for the adsorption of crystal violet dye. J. Mol. Liq., Vol.(323), PP. 115034, 2021.

[5] A. Khanam, F. Nadeem, S.M. Praveena and U. Rashid. Removal of dyes using alginated, calcinized and hybrid materials–A comprehensive review. Int. j. chem. biol. sci., Vol.(12), PP. 130-140, 2017.

[6] M.A. Dutt, M.A. Hanif, F. Nadeem and H.N. Bhatti, A review of advances in engineered composite materials popular for wastewater treatment. J. Environ. Chem. Eng.,Vol.(8), PP. 104073, 2020.

[7] S. Banerjee, M.C. Chattopadhyaya, Adsorption characteristics for the removal of a toxic dye, tartrazine from aqueous solutions by a low cost agricultural by-product. Arab. J. Chem., Vol.(10), PP. 1629-1638, 2017.

[8] Y. Li, T. Wang, S. Zhang, Y. Zhang, L. Yu and R. Liu, Adsorption and electrochemical behavior investigation of methyl blue onto magnetic nickel-magnesium ferrites prepared via the rapid combustion process. J. Alloys Compd.,Vol.(885), PP. 160969, 2021.

[9] B. Priyadarshini, T. Patra and T.R. Sahoo, Alloys, An efficient and comparative adsorption of Congo red and Trypan blue dyes on MgO nanoparticles: Kinetics, thermodynamics and isotherm studies. J. Magnes. Alloy., Vol. 9(12), PP. 478-488, 2021.

[10] C.T. Tovar, A. Villabona and Á. D. Gonzalez, Adsorption of azo-anionic dyes in a solution using modified coconut (Cocos nucifera) mesocarp: Kinetic and equilibrium study. Water, vol. 13(10), PP. 1382, 2021.

[11] A.A. Ali, S.A. Shama, A.S. Amin and S.R. EL-Sayed, Synthesis and characterization of ZrO_2/CeO_2 nanocomposites for efficient removal of Acid Green 1 dye from aqueous solution. Mater. Sci. Eng. B:, Vol.(269), PP. 115167, 2021.

[12] A.A. Ali, I.S. Ahmed, A.S. Amin and M.M. Gneidy, Auto-combustion fabrication and optical properties of zinc oxide nanoparticles for degradation of reactive red 195 and methyl orange dyes. J Inorg Organomet Polym Mater, Vol.(31), PP. 3780-3792, 2021.

[13] A.A. Ali, E.A. El Fadaly and N.M. Deraz, Auto-combustion fabrication, structural, morphological and photocatalytic activity of CuO/ZnO/MgO nanocomposites. Mater. Chem. Phys., Vol.(270), PP. 124762, 2021.

[14] K. Zhang, R. He, C. Xie, G. Wang, G. Ding, M. Wang, W. Song and D. Fang, Photosensitive ZrO_2 suspensions for stereolithography. Ceram. Int., Vol. 45(9), PP. 12189-12195, 2019.

[15] S. Li, Z. Xie, W. Xue, Microstructure and mechanical properties of zirconia ceramics consolidated by a novel oscillatory pressure sintering. Ceram. Int., Vol. 41(8), PP. 10281-10286, 2015.

[16] G. Soon, B. P. Murphy, K.W. Lai, S.A. Akbar, Review of zirconia-based bioceramic: Surface modification and cellular response. Ceram. Int., Vol. 42(11), PP. 12543-12555, 2016.

[17] X. Liu, T. Wang, J. Liu, F. Jiang, H. Tang, G. Feng, W. Jiang, Preparation, characterization and growth mechanism of ZrO_2 nanosheets. Ceram. Int., Vol. 46(4), PP. 4864-4869, 2020.

[18] F. Davar, N. Shayan, A. H. Najafabadi, V. Sabaghi and S.J. Hasani, Development of ZrO_2-MgO nanocomposite powders by the modified sol-gel method. Int. J. Appl. Ceram. Technol., Vol.(14), PP. 211-219, 2017.

[19] P. Tamilselvi, A. Yelilarasi, M. Hema and R.J. Anbarasan, Synthesis of hierarchical structured MgO by sol-gel method. Nano Bulletin, Vol(2), PP. 130106, 2013.

[20] A. Thakur, R. R. Singh and P.B. Barman, Structural and magnetic properties of La^{3+} substituted strontium hexaferrite nanoparticles prepared by citrate precursor method. J. Magn. Magn. Mater.,Vol.(326), PP. 35-40, 2013.

[21] A. H. Najafabadi, R. Mozaffarinia and A. Ghasemi, Microstructural Characteristics and Magnetic Properties of Al-Substituted Barium Hexaferrite Nanoparticles Synthesized by Auto-Combustion Sol–Gel Processing. J. Supercond. Nov. Magn., Vol. 28(9), PP. 2821-2830, 2015.

[22] A. A. Derbalah, M.M. Elsharkawy, A. Hamza and A. El-Shaer, Resistance induction in cucumber and direct antifungal activity of zirconium oxide nanoparticles against Rhizoctonia solani, Vol.(157), PP. 230-236, 2019.

[23] B. Sathyaseelan, E. Manikandan, I. Baskaran, K. Senthilnathan, K. Sivakumar, M. K. Moodley, R. Ladchumananandasivam and M. Maaza, Studies on structural and optical properties of ZrO_2 nanopowder for opto-electronic applications. J. Alloys Compd., Vol.(694), PP. 556-559, 2017.

[24] A. Arjun, A. Dharr, T. Raguram and K.S. Rajni, Study of Copper Doped Zirconium Dioxide Nanoparticles Synthesized via Sol–Gel Technique for Photocatalytic Applications. J Inorg Organomet Polym Mater.,Vol. 30(12), PP. 4989-4998, 2020.

[25] M.B. Elinski, P. LaMascus, L. Zheng, A. Jackson, R.J. Wiacek and R.W. Carpick, Cooperativity between zirconium dioxide nanoparticles and extreme pressure additives in forming protective tribofilms: toward enabling low viscosity lubricants. Tribol. Lett., Vol. 68(4), PP. 1-17, 2020.

[26] S. Medhi, S. Chowdhury, A. Kumar, D.K. Gupta, Z. Aswal and J.S. Sangwai, Engineering, Zirconium oxide nanoparticle as an effective additive for non-damaging drilling fluid: A study through rheology and computational fluid dynamics investigation. J. Pet. Sci. Eng., Vol.(187), PP. 106826, 2020.

[27] S. Z. Ajabshir and M. S. Niasari, A Sonochemical-Assisted Synthesis of Pure Nanocrystalline Tetragonal Zirconium Dioxide Using Tetramethylethylenediamine. Int. J. Appl. Ceram. Technol.,Vol.11(4), PP. 654-662, 2014.

[28] A.A. Ali, S.R. El-Sayed, S.A. Shama, T.Y. Mohamed and A.S. Amin, Fabrication and characterization of cerium oxide nanoparticles for the removal of naphthol green b dye. Desalination Water Treat., Vol.(204), PP. 124-135, 2020.

[29] D.F. Latona, Kinetic study of the discoloration of crystal violet dye in sodium hydroxide medium. J Chem Appl Chem Eng 2, 2018 .

[30] R. Foroutan, S.J. Peighambardoust, S.H. Peighambardoust, M. Pateiro and J.M. Lorenzo, Adsorption of crystal violet dye using activated carbon of lemon wood and activated carbon/Fe_3O_4 magnetic nanocomposite from aqueous solutions: a kinetic, equilibrium and thermodynamic study. Molecules, Vol. 26(8), PP. 2241, 2021.

[31] R. Foroutan, S.J. Peighambardoust, S.S. Hosseini, A. Akbari and B. Ramavandi, Hydroxyapatite biomaterial production from chicken (femur and beak) and fishbone waste through a chemical less method for Cd^{2+} removal from shipbuilding wastewater. J. Hazard. Mater., Vol.(413), PP. 125428, 2021.

[32] S.K. KARIM, N. Rabuyah, A. M. Armilla and S. H. Ismail, Removal of crystal violet dye using sugarcane fiber. Trans. Sci. Technol., Vol. 2(2), PP. 11-15, 2015.

[33] M.E. Mahmoud, G.M. Nabil, M.A. Khalifa, N.M. El-Mallah and H.M. Hassouba, Effective removal of crystal violet and methylene blue dyes from water by surface functionalized zirconium silicate nanocomposite. J. Environ. Chem. Eng., Vol. 7(2), PP. 103009, 2019.

[34] I. Langmuir, The adsorption of gases on plane surfaces of glass, mica and platinum. J. Am. Chem. Soc., Vol. 40(9), pp.1361–1403, 1918.

[35] H. Freundlich, Über die adsorption in lösungen. Vol. 57(1), PP. 385-470, 1907.

[36] M. I. Temkin, Kinetics of ammonia synthesis on promoted iron catalysts. Acta phys. chem., Vol.(12), PP. 327-356, 1940.

[37] A. A. Ali, I. S. Ahmed, E. M. Elfiky, Auto-combustion synthesis and characterization of iron oxide nanoparticles (α-Fe_2O_3) for removal of lead ions from aqueous solution. J Inorg Organomet Polym Mater ., Vol.(31), PP. 384-396, 2021.

[38] P. Sun, C. Hui, R. A. Khan, J. Du, Q. Zhang and Y. Zhao, Efficient removal of crystal violet using Fe_3O_4-coated biochar: the role of the Fe_3O_4 nanoparticles and modeling study their adsorption behavior. Sci. Rep.,Vol. 5(1), PP. 1-12, 2015.